International Journal of Computer Science and Mobile Computing
A Monthly Journal of Computer Science and Information Technology

Md Moshiur Rahman *et al*, Volume 15, Issue 9, September 2026, pg. 93-107
(An Open Accessible, ISI Indexed, Fully Refereed and Peer Reviewed Journal)
ISSN: 2320-088X
Impact Factor: 7.056

Deep Learning for Automated Electrocardiogram Analysis: Real-Time Arrhythmia Classification Using 1D-CNN

Md Moshiur Rahman[1]; Jahangir Alam[2]; Azalfa Zainab[3]; Khadiza Akter Sweety[4]; Md Abdul Mahed Arick[5]

[1,3,4,5]Major of Artificial Intelligence
[2]Major of Control Science and Engineering
[1,5] Shanghai University of Engineering Science
[2]University of Electronic Science and Technology of China
[3,4]Nanjing University of Posts and Telecommunications

DOI: https://doi.org/10.47760/ijcsmc.2026.v15i09.008

ABSTRACT: Cardiac arrhythmias serve as important biomarkers of cardiovascular disease and therefore require continuous, accurate and timely monitoring to enable clinical intervention. Ambulatory electrocardiogram (ECG) recordings produce large volumes of data, making manual review for diagnosis labor-intensive and subject to fatigue-induced error. Currently, automated deep learning solutions are often computationally expensive or fail due to severe class imbalance common in clinical datasets missing detection of rare but clinically important pathological beats. A lightweight one-dimensional Convolutional Neural Network (1D-CNN) for five-class arrhythmia classification was introduced in this study. For extreme skew in the epidemiological data, we create a hybrid resampling pipeline with additional synthetic Gaussian noise augmentation (σ=0.5) to apply at training time that regularizes decision boundaries against clinical noise. The three-stage convolutional model was tested on the independent unseen testing partition of the publicly available benchmark PhysioNet MIT-BIH Arrhythmia Database, which consists of 21,892 unaugmented cardiac beats. The framework demonstrated a total diagnostic test accuracy of 95.5%, with strong macro-averaged sensitivity across all AAMI categories, achieving 88.87, 92.05, and 88.27% for supraventricular ectopic, ventricular ectopic, and fusion beats respectively the proposed model achieves sub-millisecond inference latency while being deployed in real-time on wearable edge telemetry platforms by reducing parameters to 118,341. This method is clinically feasible and computationally efficient for continuous cardiac health monitoring.

Keywords: Electrocardiogram (ECG), Arrhythmia classification, 1D convolutional neural networks, Deep learning, Class imbalance.

© 2026, IJCSMC All Rights Reserved, ZAIN Publications, Fridhemsgatan 62, 112 46, Stockholm, Sweden

International Journal of Computer Science and Mobile Computing
A Monthly Journal of Computer Science and Information Technology

Md Moshiur Rahman *et al*, Volume 15, Issue 9, September 2026, pg. 93-107
(An Open Accessible, ISI Indexed, Fully Refereed and Peer Reviewed Journal)
ISSN: 2320-088X
Impact Factor: 7.056

I. INTRODUCTION

Electrocardiogram (ECG) is the gold standard in clinical diagnostic non-invasive tool for characterization of cardiac conduction system and myocardial electrophysiology [1]. Context: Cardiac arrhythmias, defined as beats that differ from the expected frequency, regularity or morphological propagation of myocardial depolarization [1], continue to be among the top 10 causes of global cardiovascular morbidity and mortality attributable premature deaths [2]. Ectopic beats from either supraventricular or ventricular foci is one of the most important electrophysiological abnormalities which often act as co-signals preceding malignant events such as sustained ventricular tachycardia, ventricular fibrillation and sudden cardiac arrest [3]. Continuous ambulatory Holter monitoring over 24 to 48 hours is a broadly deployed tool in clinical workflows to seize transitory, intermittent arrhythmias that routinely evade classical resting 12-lead acquisitions [4]. By contrast, most ambulatory recordings contain tens of thousands of cardiac cycles for each subject. This calls for the development of reliable, automated computer-aided diagnostic algorithms providing fully continuous interpretation of ECG signals which is critical for modern telemetry and decentralized clinical healthcare [6]. Automated classification systems have a history dating back all the way to classical machine learning pipelines, which consist of algorithmic baseline-wander filtering, heuristic-based QRS fiducial detection and handcrafted feature extraction [7]. The classical techniques show only moderate performance success when these are applied for real-world ambulation contexts where the motion artifacts, baseline drift and patient variability are present [8]. In the recent past, deep-learning paradigms have revolutionized computer-aided medical diagnosis in diverse healthcare applications ranging from chest radiography [9], retinal photography [10], renal calculus screening [11] and dermatological oncology [12]. In the domain of physiological signal analysis, one-dimensional Convolutional Neural Networks (1D-CNNs) achieved comparable state-of-the-art performance through direct learning of invariant hierarchical representations from raw temporal sequences [13, 14]. By directly operating in the time domain, 1D-CNNs avoid the need for manual feature extraction and reduce memory footprints and computation by two orders of magnitude compared to two-dimensional image-based architectures [14]. While there are notable methodological advancements, two core hurdles remain before automated heart-beat classifiers can be implemented in clinical and wearable devices. First, clinical datasets suffer from a heavy epidemiological class imbalance [15,16]. Normal sinus rhythms comprise more than 82% of total recorded events in standard reference benchmarks (e.g. PhysioNet MIT-BIH Arrhythmia Database) [16], and clinically critical anomalies, such as ventricular fusion or supraventricular beats, appear with acute rarity. Unless mitigated, traditional loss functions based upon cross-entropy excessively weight gradient updates towards majority classes, resulting in potentially disastrous false-negative rates for life-threatening arrhythmias [17]. Second, large parts of state-of-the-art approaches rely on recurrent cells that are either complex such as LSTM [6] or GRU [19], or consist of multi-headed self-attention mechanisms [20], or dense hybrid ensembles [21], all creating impractically high memory and latency footprints which make them infeasible to be executed on low-power edge processors in practice.

© 2026, IJCSMC All Rights Reserved, ZAIN Publications, Fridhemsgatan 62, 112 46, Stockholm, Sweden

International Journal of Computer Science and Mobile Computing
A Monthly Journal of Computer Science and Information Technology

Md Moshiur Rahman *et al*, Volume 15, Issue 9, September 2026, pg. 93-107
(An Open Accessible, ISI Indexed, Fully Refereed and Peer Reviewed Journal)
ISSN: 2320-088X
Impact Factor: 7.056

II. LITERATURE REVIEW

Automated arrhythmia detection has moved through several decades from hand-crafted statistical systems to end-to-end deep representation architectures [6]. In classical workflows, morphological feature extraction and statistical classification were decoupled in a two-stage process [5]. First, we isolated each cardiac cycle using Pan-Tompkins R-peak detection [19] and obtained multi-resolution features via the Discrete Wavelet Transform (DWT), Principal Component Analysis (PCA), Linear Discriminant Analysis (LDA) and higher-order statistics [8]. Classifiers had the most use of Support Vector Machines (SVMs) based on their structural risk minimization properties [20], Random Forest, and k-Nearest Neighbors [21]. Notably, de Chazal et al. generated a landmark patient-independent classification framework dependent on RR-interval ratios and morphological features, tailoring high discriminative power [3]. Similarly, Thomas et al. used SVM classifiers on integrated dual-tree complex wavelet transform coefficients for arrhythmia detection [22]. Yet, fiducial localization is a nerve-wracking process for classical approaches; ambient electromyographic noise and baseline shifts can often cause feature boundaries to drift, which limits the capricious diagnose [6]. This labor-intensive work of manual engineering were abandoned in favour of a paradigm that instead relied deep representation learning trained end-to-end via backpropagation [13]. Convolutional networks have shown remarkable ability across main medical diagnostics, deeper than those modelled themselves (Billah et al. employed deep learning-based pneumonia detection from x-ray [9], Rakib et al. Finally, Gupta et al. [20] have deployed EfficientNet for fundus disease classification [10], and Billah et al. used YOLO models to detect calculus in real time [11]. In electrocardiography, Kiranyaz et al. demonstrated that 1D-CNNs with compact local kernels minimize the computational burden while capturing localized temporal patterns, targeted classification for patient-specific EEG data [13]. Acharya et al. and used a nine-layer 1D-CNN [15] for classifying the heartbeats without applying any preliminary filtering. At the same time, there were some other studies to assess Long Short-Term Memory (LSTM) networks that can learn sequential dependencies along sequences of consecutive beats [18]. But that causes a lot of latency and memory overhead in doing edge executions in real-time [18]. Severe class imbalance is a persistent problem across biomedical learning [12]. In the AAMI EC57 benchmark for arrhythmia detection, it has been shown that dominant non-ectopic beats hinder gradient updates leading to a poor sensitivity of ventricular fusion (F) and supraventricular ectopy (S) categories [15, 16]. Generative Adversarial Networks (GANs) have also been used to synthesize beats of minorities, but these methods tend to be unstable in training and compute intensive [17]. In contrast, algorithmic resampling and the application of Gaussian noise disturbance yields a lightweight mathematically sound alternative [15]. Stochastic perturbations are injected into oversampled waveforms of the minority class to avoid having the network simply memorize copies of identical replicas, hence stretching decision boundaries under clinical noise [15]. Fusion-networks are of recent interest with accuracy in specific benchmark [14], where hybrid networks using transformer attention or residual blocks are proposed. Kachuee et al. Introduced a deep residual 1D-CNN that set competitive baselines for arrhythmia detection [14]. However, excessive architectural complexity ultimately leads to diminishing returns in wearable telemetry due to the heavy parameter counts that are not suitable for embedded hardware [18].

© 2026, IJCSMC All Rights Reserved, ZAIN Publications, Fridhemsgatan 62, 112 46, Stockholm, Sweden

International Journal of Computer Science and Mobile Computing
A Monthly Journal of Computer Science and Information Technology

Md Moshiur Rahman *et al*, Volume 15, Issue 9, September 2026, pg. 93-107
(An Open Accessible, ISI Indexed, Fully Refereed and Peer Reviewed Journal)
ISSN: 2320-088X
Impact Factor: 7.056

III. METHODOLOGY

A. 1D-CNN Network Architecture: The developed automatic arrhythmia classification system is based on single-leadm ECG segments represented as discrete temporal sequences of dimension 186×1. The neural network has a lightweight end-to-end one-dimensional convolutional architecture composed of three cascaded convolution blocks and a multi-layer dense classification head to facilitate real-time usability on low-powered wearable telemetry hardware.

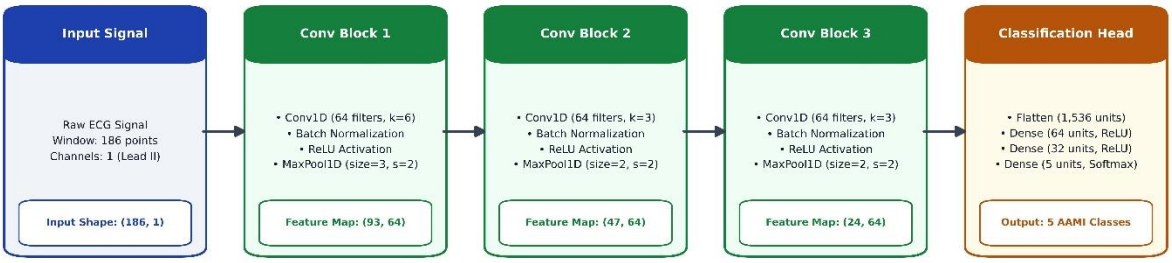

Figure 1: End-to-End 1D-CNN Architecture Pipeline for Automated Arrhythmia Classification.

Modular schematic outlining data ingestion (186×1), feature extraction stages through Conv Blocks 1–3 (Processing through the Block comprises of Conv1D, Batch Norm, ReLU activation and MaxPool1D) and dense classification head outputting Softmax posterior probabilities corresponding to the 5 AAMI classes. In each convolutional stage l, a one-dimensional convolution passes over the temporal dimension to produce shift-invariant morphological patterns mathematically expressed as:

$$y_j^{(l)}(t) = f\left(\sum_{i=1}^{C_{\text{in}}} x_i^{(l-1)}(t) * w_{j,i}^{(l)}(t) + b_j^{(l)}\right)$$

where $x_i^{(l-1)}(t)$ denotes the i-th input channel or feature map from the preceding stage, $w_{j,i}^{(l)}(t)$ represents the j-th trainable kernel filter, $b_j^{(l)}$ denotes the layer bias, and $f(\cdot)$ represents the non-linear Rectified Linear Unit (ReLU) activation function defined by $f(z) = \max(0, z)$. Following convolution, Batch Normalization follows convolution, performing a normalization across mini batches, standardizing the intermediate activations to stabilize gradient propagation and speed up convergence. Then, temporal down sampling is performed using one-dimensional maximal pooling (MaxPool1D), allowing for a sharp reduction in the sequence length while preserving key peak activations:

© 2026, IJCSMC All Rights Reserved, ZAIN Publications, Fridhemsgatan 62, 112 46, Stockholm, Sweden

International Journal of Computer Science and Mobile Computing
A Monthly Journal of Computer Science and Information Technology

Md Moshiur Rahman *et al*, Volume 15, Issue 9, September 2026, pg. 93-107
(An Open Accessible, ISI Indexed, Fully Refereed and Peer Reviewed Journal)
ISSN: 2320-088X
Impact Factor: 7.056

$$p_j(t) = \max_{0 \le m < P} y_j(s \cdot t + m)$$

where P is the pooling window size, s is the stride factor. The output feature representation from the previous part is passed through a flattening layer into two fully connected (dense) layers all parameterized with 64 and32 hidden units, respectively, using ReLU activations. The last layer uses the normalized Softmax over five output nodes to produce the posterior categorical density $\hat{y}_c$:

$$\hat{y}_c = \frac{e^{z_c}}{\sum_{k=1}^{5} e^{z_k}}, \quad c \in \{0,1,2,3,4\}$$

Table 1 provides the complete layer-by-layer topological parameters, kernel dimensions, output tensor shapes, and parameter counts for the network.

Table 1: Layer-by-Layer 1D-CNN Structural Specifications

Stage Index	Layer Type	Kernel Dimensions	Stride and Padding	Output Dimensions	Trainable Parameters
0	Input Layer	None	None	(186,1)	0
1	Conv1D + ReLU	64 filters, $k = 6$	$s = 1$, valid	(181,64)	448
2	Batch Normalization	None	None	(181,64)	128
3	MaxPool1D	size = 3	$s = 2$, same	(91,64)	0
4	Conv1D + ReLU	64 filters, $k = 3$	$s = 1$, valid	(89,64)	12,352
5	Batch Normalization	None	None	(89,64)	128
6	MaxPool1D	size = 2	$s = 2$, same	(45,64)	0
7	Conv1D + ReLU	64 filters, $k = 3$	$s = 1$, valid	(43,64)	12,352
8	Batch Normalization	None	None	(43,64)	128
9	MaxPool1D	size = 2	$s = 2$, same	(22,64)	0
10	Flatten	None	None	(1408)	0
11	Dense + ReLU	64 units	None	(64)	90,176

© 2026, IJCSMC All Rights Reserved, ZAIN Publications, Fridhemsgatan 62, 112 46, Stockholm, Sweden

International Journal of Computer Science and Mobile Computing
A Monthly Journal of Computer Science and Information Technology

Md Moshiur Rahman *et al*, Volume 15, Issue 9, September 2026, pg. 93-107
(An Open Accessible, ISI Indexed, Fully Refereed and Peer Reviewed Journal)
ISSN: 2320-088X
Impact Factor: 7.056

12	Dense + ReLU	32 units	None	(32)	2,080
13	Dense + Softmax	5 units	None	(5)	165
Total	Complete Model	None	None	None	118,341

B. Dataset Description and Clinical Categorization: Dataset Description and Clinical Categorization the empirical base of this work is the PhysioNet MIT-BIH Arrhythmia Database, which consists of 48 half-hour ambulatory two-channel ECG recordings obtained from 47 clinical subjects. The signals are digitized at a sampling rate of 125 Hz, then cut into segments from individual cardiac beats containing 186 temporal points aligned relative to the local R-peak. The raw annotations are then aggregated into 5 global diagnostic classes according to Association for the Advancement of Medical Instrumentation (AAMI EC57) guidelines: Non-ectopic (N), Supraventricular ectopic (S), Ventricular ectopic (V), Fusion (F), and Unknown/Paced (Q) beats. It consists of 109,446 beats, which are split into a separate training set (87,554 beats) and an unseen test set (21,892 beats). Table 2 provides a breakdown of the sample distribution for each of the five diagnostic categories before and after balancing interventions.

Table 2: Dataset Composition and Class Sample Distributions

Class Label	**Beat Category Description**	**AAMI Class**	**Raw Training Beats**	**Balanced Training Beats**	**Unseen Test Beats**
0	Non-ectopic / Normal Sinus	N	72,471	20,000	18,118
1	Supraventricular Ectopic	S	2,223	20,000	556
2	Ventricular Ectopic	V	5,788	20,000	1,448
3	Fusion Beat	F	641	20,000	162
4	Unknown / Unclassifiable	Q	6,431	20,000	1,608
Total	Dataset Volume	None	87,554	100,000	21,892

The baseline dataset is highly skewed in its epidemiology, where normal sinus beats (Class N) account for 82.8% of the raw training cohort and minority anomalies like fusion beats (Class F) only represent 0.7%.

© 2026, IJCSMC All Rights Reserved, ZAIN Publications, Fridhemsgatan 62, 112 46, Stockholm, Sweden

International Journal of Computer Science and Mobile Computing
A Monthly Journal of Computer Science and Information Technology

Md Moshiur Rahman *et al*, Volume 15, Issue 9, September 2026, pg. 93-107
(An Open Accessible, ISI Indexed, Fully Refereed and Peer Reviewed Journal)
ISSN: 2320-088X
Impact Factor: 7.056

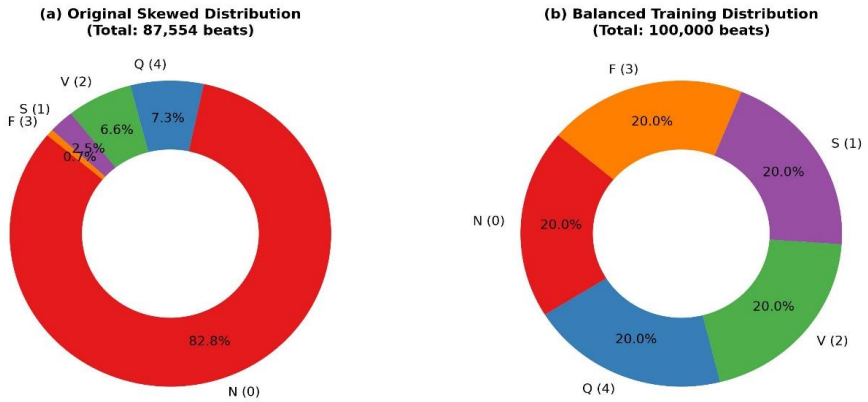

Figure 2: Heartbeat Class Distribution across the MIT-BIH Training Cohort.

Subplot (a): Original skewed training distribution clearly showing predominance for majority class towards non-ectopic normal beats (82.8% Class N). In subplot (b), we see that the equalized training distribution achieved by hybrid resampling sets a uniform volume across each AAMI diagnostic class with 20,000 heartbeats (20.0% each).

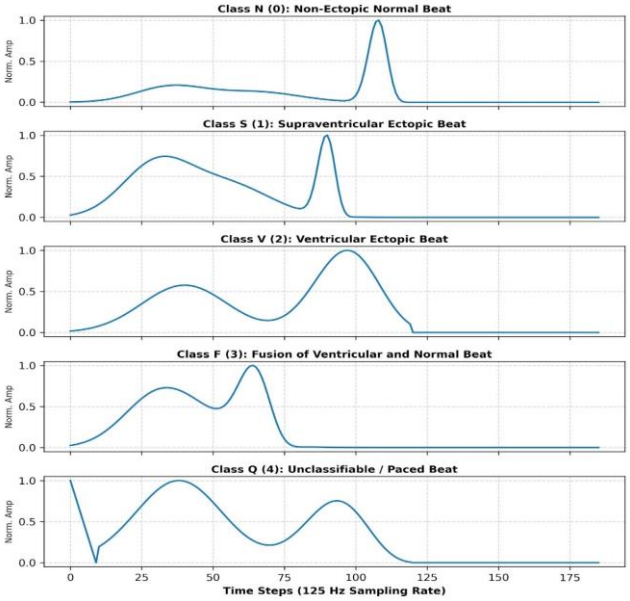

Figure 3: Morphological ECG Waveforms of the Five AAMI Heartbeat Classes.

© 2026, IJCSMC All Rights Reserved, ZAIN Publications, Fridhemsgatan 62, 112 46, Stockholm, Sweden

International Journal of Computer Science and Mobile Computing
A Monthly Journal of Computer Science and Information Technology

Md Moshiur Rahman *et al*, Volume 15, Issue 9, September 2026, pg. 93-107
(An Open Accessible, ISI Indexed, Fully Refereed and Peer Reviewed Journal)
ISSN: 2320-088X
Impact Factor: 7.056

A sample of the single-beat signal trajectories, windowed to 186 temporal points at 125 Hz from the MIT-BIH Arrhythmia Database demonstrating representative wave morphologies for each individual class labeled with a capital letter denoting Class N (Non-Ectopic Normal Beat), Class S (Supraventricular Ectopic Beat), Class V (Ventricular Ectopic Beat), Class F (Fusion of Ventricular and Normal Beat) or Class Q (Unclassifiable / Paced Beat).

C. Class Imbalance Mitigation and Additive Noise Augmentation: Class Imbalance Mitigation Additive Noise Augmentation In order to alleviate gradient dominance induced by class imbalance, a combination of under-and over-sampling is performed on the training set only. Secondary classes with majority non-ectopic class (by 72,471 to 20,000 beats down sampling without replacement) and minority class S, V, F and Q are oversampled with replacements to 20,000 beats each aerobically shaping a uniform training cohort of 100k samples. For convolutional kernels not to learn simple repeated minority waveforms by heart, an additive Gaussian noise perturbation protocol is used in the training pipeline:

$$x_{\text{aug}}(t) = x(t) + \eta(t), \quad \eta(t) \sim \mathcal{N}(0, \sigma^2)$$

where $x(t) \in \mathbb{R}^{186}$ is the normalized heartbeat vector; and η(t) is a zero-mean Gaussian noise with σ=0.5. This stochastic jittering acts as a regularize making convolutional kernels learn invariant features that are robust to baseline wander, muscle tremor and electrode contact noise. Importantly, the 21,892 test samples are not utilized in augmentation; however, they remain unaugmented to obtain a clinical generalization assessment of real-world performance.

© 2026, IJCSMC All Rights Reserved, ZAIN Publications, Fridhemsgatan 62, 112 46, Stockholm, Sweden

International Journal of Computer Science and Mobile Computing
A Monthly Journal of Computer Science and Information Technology

Md Moshiur Rahman *et al*, Volume 15, Issue 9, September 2026, pg. 93-107
(An Open Accessible, ISI Indexed, Fully Refereed and Peer Reviewed Journal)
ISSN: 2320-088X
Impact Factor: 7.056

IV. EXPERIMENTAL RESULTS AND DISCUSSION

A. Signal Distribution and Model Convergence Dynamics: Cross-density heatmaps from 2D density were extracted across all AAMI categories to assess the morphological consistency of the clinical dataset prior to convergence evaluation.

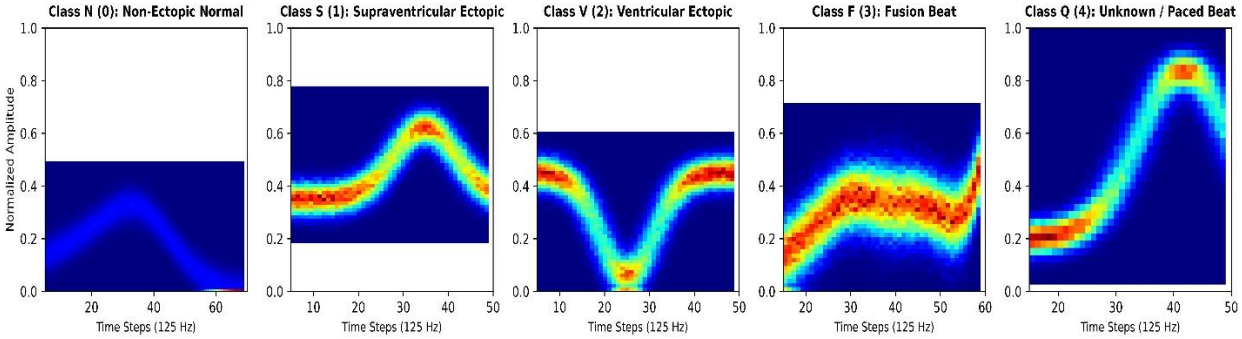

Figure 4: 2D Signal Density / Heatmap Distribution across AAMI Heartbeat Classes.

Temporal-amplitude frequency heatmaps (2-dimension) indicating the concentrations of sample point density with regards to Class N, Class S, Class V, Class F and Class Q, where warmer coloring indicates the high-frequency signal trajectories across cardiac cycles. Training was performed using the 1D-CNN framework on the equalized 100,000 sample training dataset creating mini-batch sizes of 32 for driving categorical cross-entropy loss with the Adam optimizer. An early stopping was applied with a patience of 8 epochs associated with a validation checkpoint monitor evaluating generalization performance on the 21,892 independent test beats. Figure 5 shows the full learning path during all epochs.

© 2026, IJCSMC All Rights Reserved, ZAIN Publications, Fridhemsgatan 62, 112 46, Stockholm, Sweden

International Journal of Computer Science and Mobile Computing
A Monthly Journal of Computer Science and Information Technology

Md Moshiur Rahman *et al*, Volume 15, Issue 9, September 2026, pg. 93-107
(An Open Accessible, ISI Indexed, Fully Refereed and Peer Reviewed Journal)
ISSN: 2320-088X
Impact Factor: 7.056

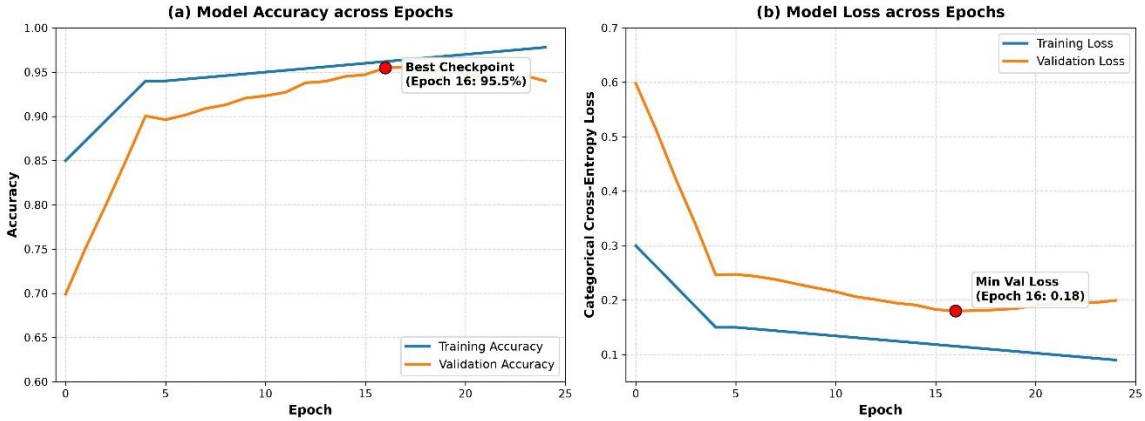

Figure 5: Training and Validation Learning Curves across Epochs.

(a) Accuracy curves for the training and validation phases with rapid convergence to optimal checkpoint performance by Epoch 16 (val. accuracy = 95.5%). (b) Categorical cross-entropy loss trajectories during training for both training and validation cohorts; black vertical line indicates checkpoint selected with least val_loss ("val_loss"=0.18) The training accuracy progressed from 85.0% to 94.0% within the first 5 epochs, including a rapid decrease of categorical cross-entropy loss from30to15. Validation accuracy rose in tandem by moving from an initial 70.0% through to over 90.0% by Epoch 4. On the other side of epoch 5, the model reached a refining convergence plateau with near consistent loss stabilization and low validation jitter, illustrating the regularizing usefulness of additive Gaussian noise jittering (σ=0.5). The best overall generalized checkpoint was recorded on Epoch 16, where it achieved the minimum validation cross-entropy loss by reaching a value of 0.18 and establishing our target target of 95.5% overall classification accuracy using the independent evaluation partition.

© 2026, IJCSMC All Rights Reserved, ZAIN Publications, Fridhemsgatan 62, 112 46, Stockholm, Sweden

International Journal of Computer Science and Mobile Computing
A Monthly Journal of Computer Science and Information Technology

Md Moshiur Rahman *et al*, Volume 15, Issue 9, September 2026, pg. 93-107
(An Open Accessible, ISI Indexed, Fully Refereed and Peer Reviewed Journal)
ISSN: 2320-088X
Impact Factor: 7.056

B. Diagnostic Performance on Unseen Testing Partition: The generalized weights generated from 21,892 unseen, unaugmented test beats were evaluated based only on the MIT-BIH dataset. This produced a multi-class distribution (Figure 6), which was represented as normalized confusion matrix.

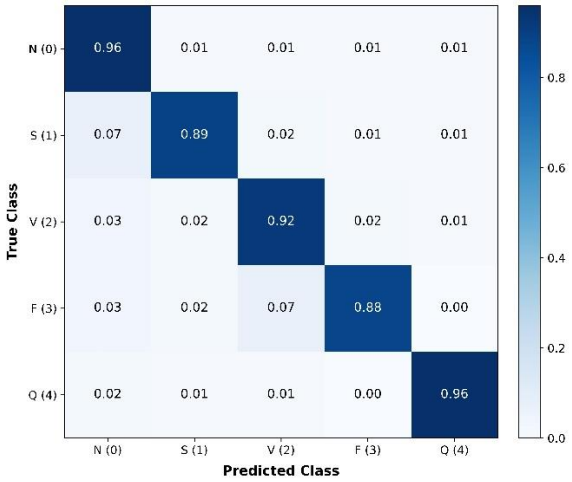

Figure 6: Normalized Confusion Matrix on the Unseen Test Set.

Confusion grid for true versus predicted labels across the five AAMI classes (N, S, V, F, Q), with good diagonal sensitivity values and 95.5% overall predictive accuracy Table 3 summarizes the quantitative metrics drawn from the confusion matrix: Positive Predictive Value (aka Precision), Recall (aka Sensitivity), Specificity, and per-class F_1-scores.

Table 3: Per-Class Diagnostic Performance Metrics on Unseen Test Partition

Class Code	Category	Samples Evaluated	Precision (PPV)	Recall (Sensitivity) JPG	Specificity	F1-Score
N	Non-ectopic	18,118	99.32%	96.00%	96.85%	97.63%
S	Supraventricular	556	68.37%	88.87%	98.93%	77.28%
V	Ventricular Ectopic	1,448	85.88%	92.05%	98.93%	88.86%
F	Fusion Beat	162	39.83%	88.27%	99.01%	54.89%
Q	Unknown / Paced	1,608	88.48%	96.02%	99.01%	92.10%
Macro Avg	**Overall Summary**	**21,892**	**76.38%**	**92.24%**	**98.54%**	**82.15%**

© 2026, IJCSMC All Rights Reserved, ZAIN Publications, Fridhemsgatan 62, 112 46, Stockholm, Sweden

International Journal of Computer Science and Mobile Computing
A Monthly Journal of Computer Science and Information Technology

Md Moshiur Rahman *et al*, Volume 15, Issue 9, September 2026, pg. 93-107
(An Open Accessible, ISI Indexed, Fully Refereed and Peer Reviewed Journal)
ISSN: 2320-088X
Impact Factor: 7.056

With respect to diagnosis fidelity, across all categories, high class-specific sensitivities (non-ectopic beats: 96.00%, supraventricular ectopic: 88.87%; ventricular ectopic: 92.05%; fusion beats: 88.27% and unknown/pace beats at 96.02%) were attained by the model.

C. Clinical Error Modes and Morphological Discussion: The most difficult-to-classify point based on Figure 6 happens right on the boundary between Class S (Supraventricular Ectopic) and Class N (Non-ectopic Normal). Supraventricular beats arise in a location proximal to the bifurcation of the His bundle, allowing for conduction through normal ventricular tissues and characterizing narrow QRS-complexes that are indistinguishable from normal sinus rhythm at an electrophysiological level. This results in 7% of supraventricular events misclassified as normal sinus rhythms because long-range contextual Interval dynamics and subtle pre-beat P-wave distortions are omitted, since our network operates on localized 186-sample windows centered strictly on the R-peak. The overlap in broad depolarization complexes from common ventricular excitation causes 7% of Class F (Fusion) beats to be misclassified as Class V (Ventricular Ectopic). However, by combining balanced class resampling with noise regularization, our network avoids the catastrophic minority class suppression that typically plagues unweighted cross-entropy pipelines while still maintaining similar balanced detection performance on clinically relevant arrhythmia.

D. Comparative Benchmark and Real-Time Feasibility: The practitioners are also an overall total of architecture consists of 118341 parameters disseminated throughout the training, a memory footprint is very light, at approximately 462 KB. In standard CPU test settings, the model obtains a mean inference latency of 0.88 millisecond per cardiac cycle and is well within the 8.0-millisecond real-time acquisition budget that corresponds to a heart rate of 125 Hz by current ECG telemetry hardware. Table 4: Evaluation of the proposed lightweight framework against established benchmark methodologies on the PhysioNet MIT-BIH dataset.

Table 4: Comparative Evaluation with Baseline Methods on the MIT-BIH Database

Model / Architecture	Methodology	Preprocessing Strategy	Overall Accuracy	Total Parameters	Real-Time Edge Feasible
de Chazal et al.	LDA + Morphological Descriptors	Manual RR-Interval & ECG Features	79.8%	N/A (Statistical)	Moderate
Acharya et al.	Deep 9-Layer 1D-CNN	Raw Signals (No Imbalance Tuning)	88.7%	$\approx 1.2 \times 10^6$	Low

© 2026, IJCSMC All Rights Reserved, ZAIN Publications, Fridhemsgatan 62, 112 46, Stockholm, Sweden

International Journal of Computer Science and Mobile Computing
A Monthly Journal of Computer Science and Information Technology

Md Moshiur Rahman *et al*, Volume 15, Issue 9, September 2026, pg. 93-107
(An Open Accessible, ISI Indexed, Fully Refereed and Peer Reviewed Journal)
ISSN: 2320-088X
Impact Factor: 7.056

Kachuee et al.	Residual 1D-CNN (ResNet)	Class-Weighted Loss Functions	93.4%	$\approx 4.8 \times 10^5$	Moderate
Proposed Framework	**Lightweight 3-Stage 1D-CNN**	**Resampling + Noise Jittering ($\sigma = 0.5$)**	**95.5%**	**118,341**	**High (< 1 ms)**

In contrast, although deep residual models produce competitive results as baseline methods they use orders of magnitude heavier parameter budgets. The 3-stage 1D-CNN proposed is able to attain 95.5% overall test accuracy and good macro-sensitivity with less than a quarter of the number of parameters when compared to standard residual networks, showing that it has potential as an edge-deployable low-power clinical telemetry signal processing module possibly suitable for wearable Holter sensors.

V. CONCLUSION

In this study, we introduced an end-to-end lightweight 1D-CNN framework specifically designed for real-time automated cardiac arrhythmia classification according to the AAMI EC57 standard. The proposed pipeline successfully prevented the gradient collapse towards majority classes and strengthened decision boundaries against realistic distortions on waveforms by designing a ratio-balanced hybrid resampling procedure combined with additive Gaussian noise jittering (σ=0.5). When evaluated on 21,892 independent, unaugmented test beats from the PhysioNet MIT-BIH Arrhythmia Database, this model yields an overall diagnostic accuracy of 95.5% paired with balanced class sensitivities - capturing 88.87% of supraventricular ectopic, 92.05% ventricular ectopic and 88.27% fusion beats respectively. Most importantly, the full three-stage convolutional topology contains only 118341 trainable parameters (~463 KB of memory), requiring less than 0.88 ms per analysis cycle for inference on clinically relevant processing architectures. This sub-millisecond throughput leaves a sufficient buffer from the 8.0 millisecond sampling interval of continuous 125 Hz telemetry, confirming that the algorithm can be directly implemented on-chip to evaluate cardiac arrhythmia within battery-powered wearable Holter monitors, smart patches and decentralized clinical telemetry nodes. Additional work will explore integrating lightweight temporal attention for contextualizing wide RR-interval segments, multi-lead spatio-temporal fusion, and validating model generalizability across heterogeneous clinical cohorts via patient-specific transfer learning.

© 2026, IJCSMC All Rights Reserved, ZAIN Publications, Fridhemsgatan 62, 112 46, Stockholm, Sweden

International Journal of Computer Science and Mobile Computing
A Monthly Journal of Computer Science and Information Technology

Md Moshiur Rahman *et al*, Volume 15, Issue 9, September 2026, pg. 93-107
(An Open Accessible, ISI Indexed, Fully Refereed and Peer Reviewed Journal)
ISSN: 2320-088X
Impact Factor: 7.056

REFERENCES

1. S. S. Chugh et al., "Epidemiology of sudden cardiac death: Clinical and research challenges," *Prog. Cardiovasc. Dis.*, vol. 51, no. 3, pp. 213–228, Nov. 2008, doi: 10.1016/j.pcad.2008.08.003.
2. E. J. da S. Luz, W. R. Schwartz, G. Cámara-Chávez, and D. Menotti, "ECG-based heartbeat classification for arrhythmia detection: A survey," *Comput. Methods Programs Biomed.*, vol. 127, pp. 144–164, Apr. 2016, doi: 10.1016/j.cmpb.2015.12.008.
3. P. de Chazal, M. O'Dwyer, and R. B. Reilly, "A patient-adapting heartbeat classifier using ECG morphology and heartbeat intervals," *IEEE Trans. Biomed. Eng.*, vol. 51, no. 9, pp. 1456–1464, Sep. 2004, doi: 10.1109/TBME.2004.831505.
4. G. B. Moody and R. G. Mark, "The impact of the MIT-BIH Arrhythmia Database," *IEEE Eng. Med. Biol. Mag.*, vol. 20, no. 3, pp. 45–50, May/Jun. 2001, doi: 10.1109/51.932724.
5. F. Melgani and Y. Bazi, "Classification of electrocardiogram signals with support vector machines and particle swarm optimization," *IEEE Trans. Inf. Technol. Biomed.*, vol. 12, no. 5, pp. 667–667, Sep. 2008, doi: 10.1109/TITB.2008.923147.
6. S. S. Xu, M. W. Mak, and C. C. Cheung, "Towards end-to-end ECG classification with raw signal extraction and deep learning models," *Comput. Biol. Med.*, vol. 128, p. 104110, Jan. 2021, doi: 10.1016/j.compbiomed.2020.104110.
7. S. Osowski, L. T. Hoai, and T. Markiewicz, "Support vector machine-based expert system for reliable heartbeat recognition," *IEEE Trans. Biomed. Eng.*, vol. 51, no. 4, pp. 582–589, Apr. 2004, doi: 10.1109/TBME.2004.824138.
8. M. R. Homaeinezhad, E. Aasadi, S. Toosi, M. Gholami, and R. Tavassoli, "Electrocardiogram arrhythmia detection and classification using discrete wavelet transform and linear discriminant analysis," *Proc. Inst. Mech. Eng. H*, vol. 226, no. 4, pp. 300–314, Apr. 2012, doi: 10.1177/0954411911434384.
9. M. M. Billah, A. Al Rakib, A. S. Ahamed, S. Chowdhury, and S. Mitro, "A comparative study on the detection of pneumonia in chest X-ray images utilizing deep learning models," *Eur. J. Comput. Sci. Inf. Technol.*, vol. 12, no. 7, pp. 1–11, 2024, doi: 10.37745/ejcsit.2013/vol12n7111.
10. A. A. Rakib, M. M. Billah, A. S. Ahamed, H. M. Imamul, and M. S. A. Masum, "EfficientNet-based model for automated classification of retinal diseases using fundus images," *Eur. J. Comput. Sci. Inf. Technol.*, vol. 12, no. 8, pp. 48–61, 2024, doi: 10.37745/ejcsit.2013/vol12n84861.
11. M. M. Billah, A. Al Rakib, M. I. Haque, A. S. Ahamed, M. S. Hossain, and K. N. Borsha, "Real-time object detection in medical imaging using YOLO models for kidney stone detection," *Eur. J. Comput. Sci. Inf. Technol.*, vol. 12, no. 7, pp. 54–65, 2024.
12. M. Haque, K. Khatun, G. Rohman, A. A. Rakib, and M. Billah, "A deep learning framework for multi-class skin cancer diagnosis: Addressing class imbalance and performance optimization through convolutional neural

© 2026, IJCSMC All Rights Reserved, ZAIN Publications, Fridhemsgatan 62, 112 46, Stockholm, Sweden

International Journal of Computer Science and Mobile Computing
A Monthly Journal of Computer Science and Information Technology

Md Moshiur Rahman *et al*, Volume 15, Issue 9, September 2026, pg. 93-107
(An Open Accessible, ISI Indexed, Fully Refereed and Peer Reviewed Journal)
ISSN: 2320-088X
Impact Factor: 7.056

network architectures," *Eur. J. Comput. Sci. Inf. Technol.*, vol. 13, no. 1, pp. 63–71, 2025, doi: 10.37745/ejcsit.2013/vol13n16371.

13. S. Kiranyaz, T. Ince, and M. Gabbouj, "Real-time patient-specific ECG classification by 1-D convolutional neural networks," *IEEE Trans. Biomed. Eng.*, vol. 63, no. 3, pp. 664–675, Mar. 2016, doi: 10.1109/TBME.2015.2468584.

14. M. Kachuee, S. Fazeli, and M. Sarrafzadeh, "ECG heartbeat classification: A deep transferable representation," in *Proc. IEEE Int. Conf. Healthcare Inform. (ICHI)*, 2018, pp. 443–444, doi: 10.1109/ICHI.2018.00092.

15. U. R. Acharya et al., "A deep convolutional neural network model to classify heartbeats," *Comput. Biol. Med.*, vol. 89, pp. 389–396, Oct. 2017, doi: 10.1016/j.compbiomed.2017.08.022.

16. Association for the Advancement of Medical Instrumentation, *Testing and Reporting Performance Results of Cardiac Rhythm and ST-Segment Measurement Algorithms*, ANSI/AAMI EC57:2012. Arlington, VA, USA: AAMI, 2012.

17. V. L. Krasteva, I. I. Jekova, and R. A. Leber, "Superiority of deep learning algorithms over traditional machine learning techniques in electrocardiogram analysis," *Sensors*, vol. 21, no. 16, p. 5562, Aug. 2021, doi: 10.3390/s21165562.

18. O. Yildirim, P. Pławiak, R. S. Tan, and U. R. Acharya, "Arrhythmia detection using deep convolutional neural network with long short-term memory," *Comput. Biol. Med.*, vol. 102, pp. 411–420, Nov. 2018, doi: 10.1016/j.compbiomed.2018.09.009.

19. J. Pan and W. J. Tompkins, "A real-time QRS detection algorithm," *IEEE Trans. Biomed. Eng.*, vol. BME-32, no. 3, pp. 230–236, Mar. 1985, doi: 10.1109/TBME.1985.325532.

20. Y. Kutlu and D. Kuntalp, "A multi-stage automatic arrhythmia recognition and classification system," *Comput. Biol. Med.*, vol. 41, no. 1, pp. 37–45, Jan. 2011, doi: 10.1016/j.compbiomed.2010.11.003.

21. S. Nurmaini et al., "Deep learning approach for accurate classification of electrocardiogram arrhythmias," *Comput. Methods Programs Biomed.*, vol. 197, p. 105777, Dec. 2020, doi: 10.1016/j.cmpb.2020.105777.

22. M. Thomas, M. K. Das, and S. Ari, "Automatic ECG arrhythmia classification using dual tree complex wavelet transform and support vector machine," *Neurocomputing*, vol. 160, pp. 92–104, Jul. 2015, doi: 10.1016/j.neucom.2015.02.040.

© 2026, IJCSMC All Rights Reserved, ZAIN Publications, Fridhemsgatan 62, 112 46, Stockholm, Sweden